# AN ELECTRO-OPTIC ATTENUATOR FOR TERAHERTZ FREQUENCIES

Guillermo F. Delgado[†], Stellan W. Jacobsson[‡], Joakim F. Johansson[†]

† Department of Radio and Space Science
with Onsala Space Observatory

‡ Department of Microwave Technology

Chalmers University of Technology
S-412 96 Gothenburg
Sweden

## ABSTRACT

*At Gigahertz and Terahertz frequencies the signals are commonly handled quasi-optically. Thus, a large number of devices have been developed to perform various manipulations of the signals. However, simple devices for fast and continuous power attenuation of a Gaussian beam are still lacking.*

*We have previously shown that a 100 GHz quasi-optical beam can effectively be attenuated by means of generation of excess carrier densities under photonic excitation of a semiconductor material at room temperature. The particular material used was a molecular beam epitaxy (MBE) engineered III-V semiconductor. The photonic excitation was achieved by illuminating the MBE material with an infrared LED.*

*Here, we present a further investigation of the same material into the THz region. A polarising Michelson Fourier transform spectrometer was used to characterise the material between 0.5 and 8 THz. The material was found to modulate over the region between 0.5 and 5 THz and have a modulation depth, in transmission mode, of more than 3 dB between 0.5 and 2.5 THz.*

## 1. INTRODUCTION

Presently the technology of sub-millimeter waves has been pushed towards the *last frontier: i.e.* the Terahertz range. This development has been partly supported by natural extensions of the mature techniques developed and improved for the sub-millimeter wave range.

Due to the short wavelengths at the THz frequencies, and high losses in conventional guided wave systems, there has been a need to use extensively quasi-optical techniques, and this has been done with a lot of success. In fact almost all the signal processing at these frequencies is done quasi-optically.

One particular area of the quasi-optical handling that lacks a good and simple solution (at these frequencies as well as at lower frequencies), is continuous attenuation of a Gaussian beam. There are some solutions to this problem, but they involve the use of interferometric devices with moving grids or reflecting planes, and while they might work quite well at lower frequencies, the sizes involved become so small at higher frequencies that a practical mechanical device becomes too difficult or expensive to manufacture.

Of course there are more crude approaches like the use of graduated filters, more or less in the same way as in the optical regime, but these solutions are not applicable if the desire is to have a continuous power control.

Recently there have been some reports of a completely quasi-optical electro-optic control of a Gaussian beam [1, 2] at millimeter wavelengths (70 and 100 GHz). The material used in both cases is a molecular beam epitaxy (MBE) engineered III-V semiconductor [3]. Since the physical principle involved in these modulators has no theoretical limit towards the THz region we initiated a deeper study of the potential of this material as a modulator for this region of the spectrum.

## 2. THEORY

The MBE grown structure consists of 44 $In_{0.2}Ga_{0.8}As$ quantum wells (QW), each 6.5 nm thick, separated by 78 nm thick GaAs barriers. In the centre of each GaAs barrier, a Be-doped plane (*p*-type) with a sheet density of $9 \cdot 10^{16}$ $m^{-2}$ is inserted. On both sides of the QWs, using 10 nm thick spacer layers, Si-doping planes (*n*-type) with sheet densities of $3 \cdot 10^{16}$ $m^{-2}$ are inserted. The excess hole concentration locates the Fermi level sufficiently far below the electron ground state in the QWs to ensure that the QWs are essentially free from electrons under thermal equilibrium.

During electron-hole pair generation, electrons will be attracted to the QWs and the holes to the barrier region midway between the wells, resulting in their spatial separation. This spatial separation of the carriers reduces the recombination rate and thus large densities of electrons can be established in the QWs using low excitation densities.

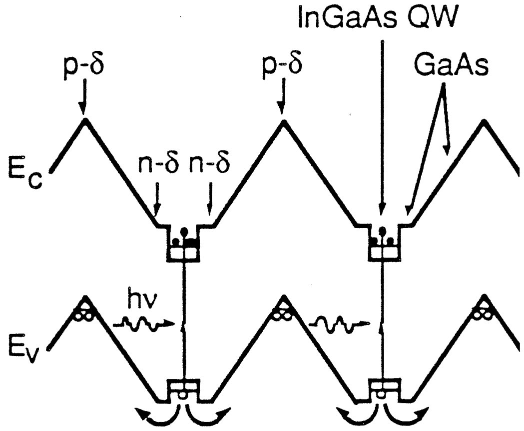

*Figure 1. Energy band diagram for the periodically doped InGaAs/GaAs MQW sample showing the spatial separation (figure kindly provided by Professor Anders Larsson).*

The structure has been described elsewhere, as well as its main properties at near IR wavelengths [3, 4, 5].

For a TEM wave propagating through a two dielectric layered medium, the ratio for the reflected and transmitted field to the incident field is given by

$$\frac{E_R}{E_0} = \frac{\Gamma_{01} + \Gamma_{12}\left(e^{-j2\kappa_1 t_1} + \Gamma_{01}\Gamma_{20}\, e^{-j2\kappa_2 t_2}\right) + \Gamma_{20}\, e^{-j2(\kappa_1 t_1 + \kappa_2 t_2)}}{1 + \Gamma_{12}\left(\Gamma_{01}\, e^{-j2\kappa_1 t_1} + \Gamma_{20}\, e^{-j2\kappa_2 t_2}\right) + \Gamma_{01}\Gamma_{20}\, e^{-j2(\kappa_1 t_1 + \kappa_2 t_2)}}\, e^{j2\kappa_0 t_1} \qquad (1)$$

$$\frac{E_T}{E_0} = \frac{(1+\Gamma_{01})(1+\Gamma_{12})(1+\Gamma_{20})}{1+\Gamma_{12}\left(\Gamma_{01}e^{-j2\kappa_1 t_1}+\Gamma_{20}e^{-j2\kappa_2 t_2}\right)+\Gamma_{01}\Gamma_{20}e^{-j2(\kappa_1 t_1+\kappa_2 t_2)}} e^{-j(\kappa_1-\kappa_0)t_1} e^{-j(\kappa_2-\kappa_0)t_2} \quad (2)$$

where $\Gamma_{01}$, $\Gamma_{12}$ and $\Gamma_{20}$ refer to the reflection coefficients at the boundaries between air (subscript 0), first dielectric (subscript 1), and second dielectric (subscript 2).

$$\Gamma_{01} = \frac{\kappa_0 - \kappa_1}{\kappa_0 + \kappa_1} = \frac{1-\sqrt{\varepsilon_1}}{1+\sqrt{\varepsilon_1}} \quad (3)$$

$$\Gamma_{12} = \frac{\kappa_1 - \kappa_2}{\kappa_1 + \kappa_2} = \frac{\sqrt{\varepsilon_1}-\sqrt{\varepsilon_2}}{\sqrt{\varepsilon_1}+\sqrt{\varepsilon_2}} \quad (4)$$

$$\Gamma_{20} = \frac{\kappa_2 - \kappa_0}{\kappa_2 + \kappa_0} = \frac{\sqrt{\varepsilon_2}-1}{\sqrt{\varepsilon_2}+1} \quad (5)$$

Here, the magnitude of the wave vector is dependent of the relative dielectric constant of the material:

$$\kappa_i = \kappa_0\sqrt{\varepsilon_i} = \kappa_0 n_i \quad (6)$$

where $n_i$ is the complex refractive index of the material.

The geometry of the problem is shown in Figure 2, together with the relevant parameters.

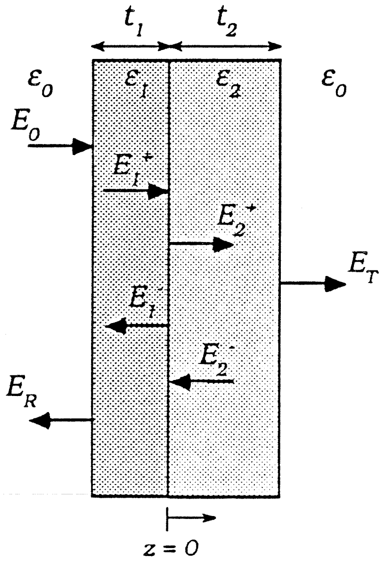

*Figure 2. Geometry of the problem with the associated electric fields and relevant parameters*

In a semiconductor material the conductivity is given as a function of the carrier density $N_e$, the electron charge $e$, the average relaxation time $T_m$, and the effective mass of the carriers $m_e^*$ (effective electron mass in GaAs):

$$\sigma = \frac{N_e e^2 \langle T_m \rangle}{m_e^*} \quad (7)$$

Relation (7) is valid provided that we assume that only electrons contribute to the charge transport (current). This holds since the mobility of holes in GaAs is nearly 20 times lower than the one for electrons.

In the active region of the semiconductor the average relaxation time, $T_m$, is a complex function of the frequency of the incident radiation, $\omega$, and the effective relaxation time, $\tau_m$.

$$\langle T_m \rangle = \frac{1}{\dfrac{1}{\tau_m} + j\omega} = \frac{\tau_m}{1+(\omega\tau_m)^2} - j\frac{\omega\tau_m^{\,2}}{1+(\omega\tau_m)^2} \qquad (8)$$

The former is just an alternative formulation of the classic Drude model for free electrons that can be applied to the doped semiconductor case, and where $\tau_m$ is defined as

$$\frac{1}{\tau_m} = \frac{1}{\tau_{life}} + \frac{1}{\tau_{coll}} \qquad (9)$$

with $\tau_{life}$ the carrier lifetime (which is of the order of milliseconds in this material [1, 6]), and $\tau_{coll}$ is the collision time for the carriers (of the order of femtoseconds in GaAs [7]). We see that since the carrier lifetime is so long in the material used, the relaxation time will be dominated by the collision time.

Combining (7) and (9), we have that the complex conductivity can be expressed as

$$\sigma(N_e,\omega) = \frac{N_e e^2}{\dfrac{m_e^*}{\tau_{coll}} + j\omega m_e^*} = \frac{N_e e^2 \tau_{coll}}{m_e^*\left[1+(\omega\tau_{coll})^2\right]} - j\frac{N_e e^2 \omega \tau_{coll}^{\,2}}{m_e^*\left[1+(\omega\tau_{coll})^2\right]} \qquad (10)$$

In a lossy dielectric the relative permittivity is given by

$$\tilde{\varepsilon}_r = \varepsilon_r - j\frac{\sigma}{\varepsilon_0\omega} \qquad (11)$$

Using (10) in (11) we can summarise our results in

$$\tilde{\varepsilon}_r(N_e,\omega) = \varepsilon_r - \frac{N_e e^2 \tau_{coll}^{\,2}}{m_e^*\varepsilon_0\left[1+(\omega\tau_{coll})^2\right]} - j\frac{N_e e^2 \tau_{coll}}{m_e^*\varepsilon_0\omega\left[1+(\omega\tau_{coll})^2\right]} \qquad (12)$$

In order to get simpler approximations of (12), we should check the value of the product $\omega\tau_{coll}$. Using $\tau_{coll}$ = 200 fs, we have that the turn-over point is close to 800 GHz, so in the low Terahertz range we have to use the complete expression.

From equations (1) to (5) and the value of the complex relative permittivity obtained in (12), it is clear that the reflection and transmission properties of the *nipi* MQW material will be functions of the semiconductor properties like scattering time, effective mass of the carriers, and relative dielectric constant of the base material. But, most important for our work, they will also be functions of the frequency and of the free carrier density. Now, assuming that we work at a fixed frequency — or rather a narrow frequency range —, we find that the optical properties of the material can be effectively changed by modulating the carrier density and this is in turn done by modulating the IR optical power incident on the *nipi* MQW structure.

## 3. MEASUREMENT TECHNIQUE

Fourier transform spectroscopy (FTS) is a well known general spectrometric method. The spectrum is obtained via a numerical Fourier transformation of a recorded interferogram obtained by a two-beam interferometer (*e.g.* Michelson) [8, 9]. The FTS concept is applicable in any part of the electromagnetic spectrum, although the majority of the spectrometers work at the longer wavelength side of the visible part of the spectrum.

The signal source is a mercury lamp, known to emit an excess of power in the millimeter and submillimeter part of the spectrum. The beam from the mercury lamp is collimated and equally divided, by wire grid polarizers, between the two arms of the interferometer. The interferogram is obtained by step-wise moving one of the mirrors in the interferometer to a large number of equidistant positions. In each position the power impinging on the detector is sampled. By numerical Fourier transformation of the interferogram the power spectrum is obtained. The total optical path length the mirror has travelled during the measurement determines the spectral resolution, whereas the distance between the sampling positions determines the maximum frequency. In order to improve the signal-to-noise ratio and to separate the signal from the background, phase modulation is used. This is accomplished by vibrating (≈ 30 Hz) the mirror (in the fixed arm of the interferometer) in order to introduce a small path length modulation. The phase modulation is wavelength dependent and creates nulls in the calculated spectra at frequencies corresponding to vibration amplitudes equal to half a wavelength (in the measurements done for this paper, the nulls are located outside the frequency range of interest). The interference signal is detected and later demodulated by a lock-in amplifier.

The particular spectrometer (Graseby SPECAC Ltd.) used in this study is of the polarising Michelson type and can be used between (approximately) 100 GHz and 30 THz. The useful spectral range is determined by the power emitted by the mercury lamp, but also on the particular detector and window materials being used. The spectrometer has a maximum obtainable resolution of 0.75 GHz (corresponding to a 0.2 m maximum travelling range of the movable interferometer arm). The sample chamber can be evacuated to avoid water vapour absorption.

The *nipi* MQW sample under test and the IR illuminator for the structure were mounted in the evacuated test compartment. By flipping a mirror, either the transmission or reflection could be measured. A Golay cell was used as a detector. A filter arrangement was used to protect the *nipi* structure from being illuminated by the UV, visible and IR emission from the mercury lamp. The measurements are differential in the sense that the transmission (or reflection) is obtained by normalizing the sample spectrum to a reference spectrum.

The reference spectra were taken without the sample, but keeping the rest of the set-up, including the protection filters in front of the sample. For the reflection reference we used a polished copper mirror (10 µm RMS).

Each one of the measured spectra comprised two independent ones; one of 20 minutes and a second one of 60 minutes, thus giving a total integration time of 80 minutes for each spectrum. The "short" spectrum was used as a reference to check any possible deviation of the "long" one. In every case the agreement between them was excellent.

The sample was measured twice: a *dark* measurement, *i.e.* the sample without any light excitation, and a *illuminated* measurement, *i.e.* the sample illuminated with an IR power density of the order of 200 Wm$^{-2}$ (100 mA forward current on a commercial IR LED: Texas Instruments TIL 31B)

# 4. RESULTS

## 4.1 Transmission

In Figure 3 we have the result of the series of measurements done in transmission mode. We can see that the modulator ceases to respond at a frequency around 5.5 THz, defining the absolute limit for this device.

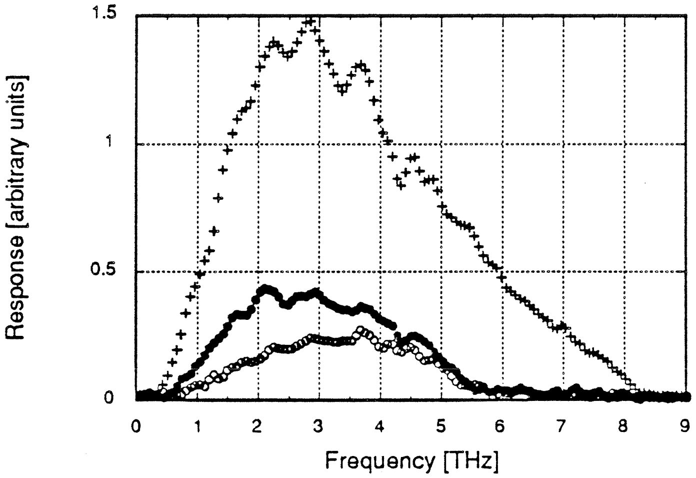

*Figure 3. Response of a nipi MQW structure to different illumination levels in transmission mode. The upper curve (crosses) represents the reference, the second one (filled circles) the dark response, and the last one (open circles) the illuminated response.*

The modulation depth for this mode is shown in Figure 4. We can see that for frequencies between 0.5 and 5 THz the device modulates more than 1 dB and for frequencies between 0.5 and 2.5 THz the modulation depth is better than 3 dB, reaching a maximum modulation depth between 5 and 6 dB in the lower frequency range.

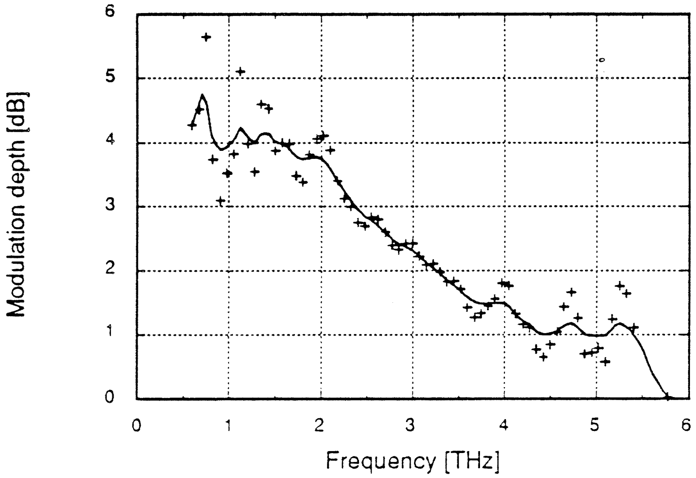

*Figure 4. Modulation depth in transmission mode for a nipi MQW structure.*

The insertion loss is shown in Figure 5 where it is possible to see that in the range where the device gives better performance (0.5 to 2.5 THz), the losses are of the order of 4-5 dB, being rather flat around the frequency range between 1 and 5 THz.

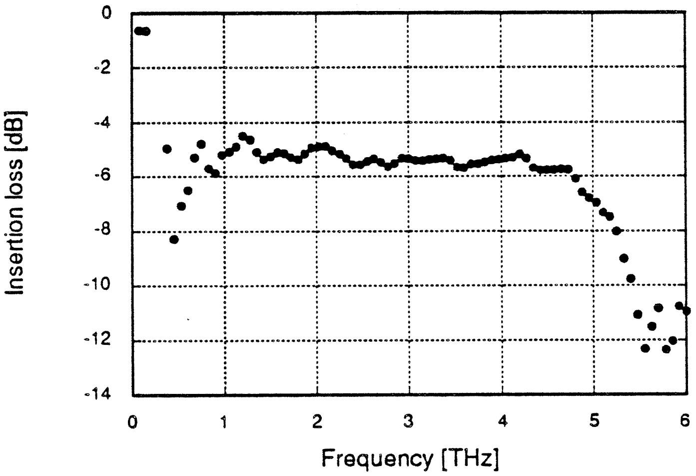

*Figure 5. Insertion loss in transmission mode for a nipi MQW structure.*

## 4.2 Reflection

Figure 6 gives the result of the series of measurements done in reflection mode. This time we cannot see a cut-off for the modulator response before the cut-off of the sensitivity of the Golay cell in the FTS. Note that in this case we have less attenuation when the sample is illuminated.

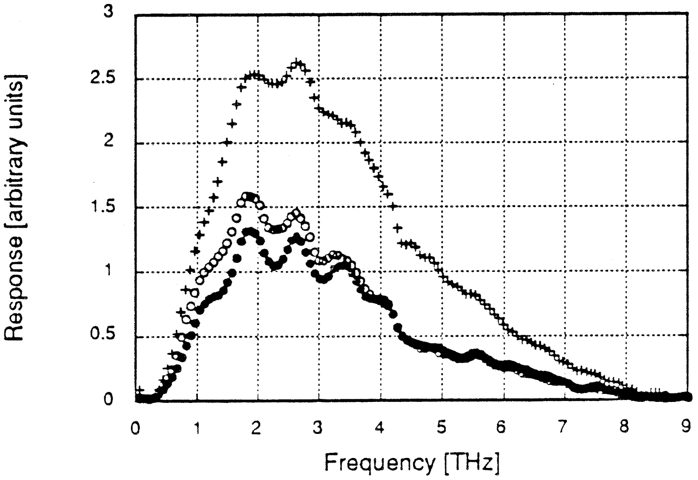

*Figure 6. Response of a nipi MQW structure to different illumination levels in reflection mode. The upper curve (crosses) represents the reference, the second one (open circles) the illuminated response, and the last one (filled circles) the dark response.*

The modulation depth observed for this mode is shown in Figure 7. It can be seen that this device does not offer that much of modulation working in reflection mode, hardly reaching 2 dB at the lower frequency side and going below 1 dB of modulation at around 1.5 THz.

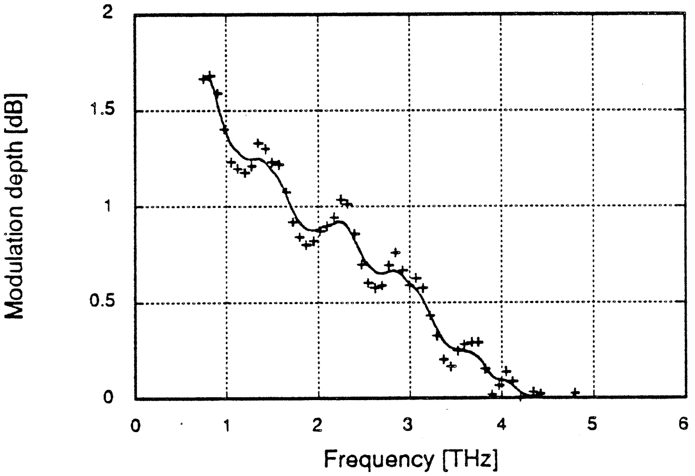

*Figure 7. Modulation depth in reflection mode for a nipi MQW structure*

Finally, the reflection loss is shown in Figure 8 where we can see that, for this mode of operation, the device offer a small advantage compared with the transmission mode since the losses are of the order of 3-4 dB.

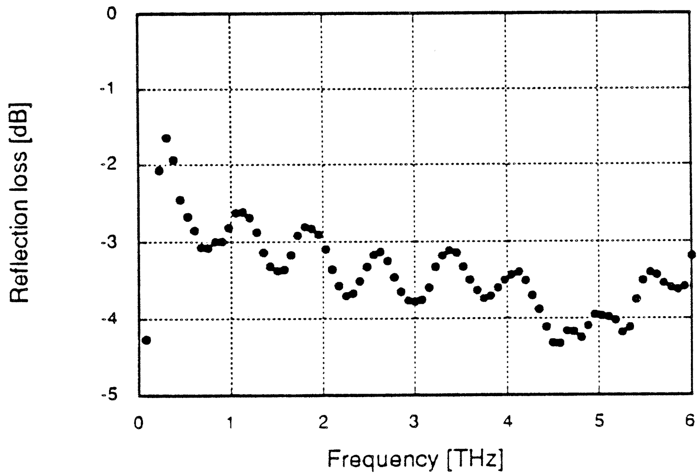

*Figure 8. Reflection loss in reflection mode for a nipi MQW structure*

## 5. DISCUSSION AND CONCLUSIONS

We have investigated the possibilities of using a *nipi* MQW engineered material as a continuously adjustable quasi-optical attenuator at Terahertz frequencies. The device achieves electro-optic modulation from 0.5 up to 5 THz and this modulation is better than 3 dB over the range of 0.5 to 2.5 THz in transmission mode.

The losses found in the material are moderately large (of the order of 4 dB) and is something that can be improved by, for example, reducing the thickness of the GaAs substrate [2].

The use of this type of material, provided that the losses can be afforded, fills a gap in the range of quasi-optical devices used for signal handling at Terahertz frequencies. The power control is achieved by the use of a commercial IR LED (TIL 31B) and very low optical power levels (6 mW @ 100 mA of forward current through the IR LED) are needed due to the long carrier lifetime inherent to this *nipi* MQW material

Possibly, the modulation depth can be improved by increasing the IR optical power density on the *nipi* MQW structure, but due to mechanical constraints in the sample holder, the distance between the sample and the IR LED was too large in our case, yielding an IR optical power density about half of the one required to generate all the free carriers available.

## 6. ACKNOWLEDGEMENTS

The authors want to thank Professor Anders G. Larsson at the Dept. of Optoelectronics and Electrical Measurements, Chalmers University of Technology (CTH), for designing the material and being a very helpful discussion partner. Dr. Thorvald Andersson at the MBE Group, Physics Dept., CTH is gratefully acknowledged for providing the MBE engineered sample.

## 7. REFERENCES

[1] G. Delgado and J. Johansson, "Electro-optic power control of a millimeter wave Gaussian beam," to be published in *Proc. Intl. Conf. on mm and sub-mm Waves and Appl.*, SPIE, San Diego, January 1994.

[2] A. Kost, L. West, T. Hasenberg, J. White, and M. Matloubian, "Optical control of microwaves with semiconductor *n-i-p-i* structures," *Appl. Phys. Lett.*, Vol. 63, No. 25, pp. 3494-3496, December 1993.

[3] A.G. Larsson and J. Maserjian, "Molecular beam epitaxy engineered III-V semiconductor structures for low-power optically addressed spatial light modulators," *Opt. Eng.*, Vol. 31, No. 7, pp. 1576-1582, July 1992.

[4] J. Maserjian, P. Andersson, B. Hancock, J. Iannelli, S. Eng, F. Grunthaner, K. Law, P. Holtz, R. Simes, L. Coldren, A. Gossard, and J. Merz, "Optically addressed spatial light modulators by MBE-grown nipi MQW structures," *Appl. Opt.*, Vol. 28, No. 22, pp. 4801-4807, November 1989.

[5] A. Larsson, and J. Maserjian, "Optically Induced Absorption Modulation in a periodically $\delta$-doped InGaAs/GaAs Multiple Quantum Well Structure," *Appl. Phys. Lett.*, Vol. 58, No. 10, pp. 1946-1948, 1991.

[6] B. Jonsson, A. Larsson, O. Sjölund, S. Wang, T. Andersson, and J. Maserjian, "Carrier Recombination in a Periodically δ-doped Multiple Quantum Well Structure," *Technical Report No. TR 92308*, Department of Optoelectronics and Electrical Measurements, Chalmers University of Technology, Gothenburg, Sweden, 1992.

[7] S. Sze, **Physics of Semiconductors Devices**, 2nd Ed., Wiley-Interscience Publication, 1981.

[8] D. Martin, "Polarising (Martin-Puplett) interferometric spectrometers for the near- and submillimeter spectra", in **Infrared and millimeter waves: Systems and components**, Vol. 6, Ed. K.J. Button, Academic Press, 1982.

[9] J. Chamberlain, **The principles of interferometric spectroscopy**, Wiley, 1979.